

3D Evaluation of PWP Development Due to Tunnel Excavation in an Over Consolidated Clay

D. L. Vettorello¹, F. A. M. Marinho¹, and P. D. G. Orlando²

¹Instituto de Geociências, Universidade de São Paulo, São Paulo, Brazil

²Instituto de Pesquisas Tecnológicas do Estado de São Paulo, São Paulo, Brazil

Email: danilo.vettorello@gmail.com

ABSTRACT: The stress relief promoted by the excavation process may induce the reduction of the pore water pressure within the soil when an undrained condition occurs. According to the magnitude of the stress relief and the initial hydrostatic pressure, the pore water pressure reduction may generate suction in the soil, thus increasing the soil shear strength. Effects of the stress relief promoted by a circular tunnel excavation process in stiff clay was investigated by means of a series of 3D numerical analyses. These analyses considered a NATM unsupported excavation advance of a shallow and small diameter tunnel in a saturated soil mass. The results highlight the development of a suction zone in front of the tunnel face where the soil shear strength is increased. The extension of this suction zone and its dissipation rate through time, however, are influenced by the soil mass coefficient of earth pressure at rest, and hydraulic conductivity, respectively.

KEYWORDS: Tunnels, 3D Numerical model, Pore water pressure development, Stress relief, Overconsolidated clay.

1. INTRODUCTION

The stress relief related with unloading events induces a negative variation of the pore water pressure in soils (Simonsen and Sorensen, 2017). Depending on the stress relief magnitude and the initial hydrostatic pore water pressure, suction may be generated in soil, bringing about a temporary improvement in soil shear strength (Vaughan and Walbancke, 1973). Underground excavations, such as those performed during tunnelling in soil masses, are practical examples of engineering works that may benefit from an increase in soil shear strength due stress relief even though excavation stability analyses rarely take this phenomenon into account.

During an ongoing excavation, the stress relief induced may not always generate suction but a pore water pressure reduction in some parts of the soil mass (Simonsen and Sorensen, 2017). Both the reduction of the pore water pressure or the occasional suction generation can benefit the soil's stability during a certain period of time (e.g. Potts et al., 1997; Kovacevic et al., 2007). Understanding the negative variations of pore water pressure due to stress relief may therefore help in the evaluation of some important phenomena as the *stand-up time* of an unsupported tunnel span (Terzaghi, 1950). The period of time that an unsupported excavation in a soil mass will support itself without any added support structure, or the *stand-up time*, may have to be related to the soil negative excess pore water pressure dissipation rate. Since the water flow of the soil mass is governed by hydraulic conductivity, the benefit soils get from the negative excess porewater pressure may last as long as the drainage process allows (e.g. Wan and Standing, 2014). For this reason, the improvement soil obtains in its shear strength due to stress relief is more significant for low permeability soil, such as clays, than it is for medium to high permeability materials, such as silty and sandy soils.

Even fully saturated soil may develop suction as a result of the stress relief caused by an excavation process. This event is related to water's physical property of being able to withstand high negative pressures, which makes soil suction maintenance during fully undrained conditions possible if the suction value is lower than the material air-entry value (e.g. Vanapalli et al., 1996). The air-entry value is the maximum negative pore water pressure a soil can sustain without desaturation occurring. In general, even with a degree of saturation higher than 90%, the effective stress concept can be applied (e.g. Terzaghi, 1923; Marinho et al., 2003).

The influence of depressed pore water pressure values in slope stability, as a result of the unloading effect of the excavation, was reported by Vaughan and Walbancke (1973). The authors described that that even after nine years of the slope excavation, the pore water pressure measured by piezometers was lower than the expected for

the ultimate equilibrium. The low negative excess pore water pressure dissipation rate was assigned as related to the extremely low permeability of the excavated material, which was London clay. The authors suggested that the slow negatives excess pore water pressure dissipation process was the main phenomenon that could delay failure of slopes in overconsolidated clays.

A similar phenomenon occurs when excavation for a tunnel is done. Davis et al. (1980) investigated the stability of shallow tunnels in soft soils and reported the negative pore pressure generation as a result of the stress relief as well as its role in excavation stability when the soil mass is under an initially and temporarily undrained condition. Moreover, a 2D numerical analysis of an excavation presented by Holt and Griffiths (1992) highlighted the role of hydraulic conductivity, drainage path length, and rate of excavation in the stability of excavations.

Using a sophisticated 2D numerical methodology Potts et al. (1997) performed parametric analyses with the aim of evaluating the behaviour of cuts in brown London clay. The study showed the effect of K_0 on pore water pressure generation, indicating that the higher the K_0 value, the higher is the negative variation of pore water pressure. It also found that the subsequent time taken for excavation collapse increased with K_0 . Moreover, the soil yielding considering high K_0 values tended to occur after larger absolute displacements as compared to those registered for small K_0 values despite the displacement rate itself increasing with K_0 raises. The study also highlighted the important role surface suction has on the stability of cuts.

Höfle et al. (2008) performed a 3D analysis to investigate how the deformation of the surrounding fine-grained soil of a tunnel is influenced by hydraulic conductivity (k) and the rate of tunnel driving. They found that the volume of the plastification zone is associated with the hydraulic conductivity in which the lower the value of k , the smaller is the plastification zone. A 3D finite element analysis was also performed by Ng and Lee (2002), investigating the behaviour of a tunnel face in London clay with soil nailing for stabilization. The authors found that the pore water pressure generated was related to soil deformation. According to the authors, the presence of soil nailing limited the negative pore water pressure generation since less shearing was induced. Finally, Schuerch and Anagnostou (2013), emphasized the importance of hydraulic-mechanical coupled analyses for tunnelling studies.

In summary, the stability of an excavation depends, *inter alia*, on the initial stress condition, the rate of excavation, and soil hydraulic conductivity. The combination of these factors can generate an undrained condition for the soil water. Meanwhile, generating a negative pore water pressure variation due to stress relief can

maintain the stability of an excavation for some time. In some cases, stress relief can lead to negative pore water pressure values, still keeping the soil in a saturated condition. All these aspects are being studied, and the phenomenology is well-defined. However, the present study presents a 3D analysis where stress relief occurs by removing a volume of ground that creates an advance of the excavation front rather than by decreasing stress on the front of the tunnel face. The presented results delimit the zone of development of the negative pore water pressure and its dissipation over time. This allows the researchers to evaluate how the negative water pressure variation is generated and how it dissipates over time. A numerical simulation of a shallow and small diameter unsupported tunnel excavation was carried out in an initially saturated soil mass of overconsolidated stiff clay. The developed numerical models were used to perform parametric analyses to evaluate the effect of the coefficient of earth pressure at rest (K_0) on the magnitude of the stress relief generated by the excavation processes. Furthermore, it also evaluated the role of the coefficient of hydraulic permeability (k) in the dissipation rate of the negative pore water pressure induced. The dissipation of the pore water pressure was compared to the soil deformation after excavation.

2. MAIN HYPOTHESIS

The model intends to evaluate the effect of the excavation process in the development of pore water pressure as well as its reverberation on the soil deformation rate. The numerical model represents a shallow, unsupported tunnel excavation advance of 1 m from a pre-existing lined, circular cross-section tunnel of 4 m diameter and 8 m depth as shown in Figure 1. The following hypothesis were assumed:

- The soil is homogeneous.
- The water table is at the surface all the time (ground water recharge).
- A pre-existing tunnel has been perfectly excavated and lined.
- The tunnel liner was considered not susceptible to deformities and is impermeable.

Information about the soil water retention curve were given, and a value of ϕ^b was established (Vettorello, 2019). The analysis uses the value of ϕ^b in the case where the stress relief induces a suction higher than the air-entry value.

3. THE 3D MODEL - STATEMENT OF THE PROBLEM

The three-dimensional geometric model was created within the software RS3 (Rocsience, 2019). The analyzes were carried out as transient and coupled, which means that the variation on pore water pressure and the volume change process over time were related and based on the Biot (1941) theory. Accompaniment is important so that it is possible that volume variations can occur both in the discharge, when negative pore pressures are generated, and during the dissipation of these pore pressures. The failure criterion adopted for the constitutive model of the soil was the Mohr-Coulomb, with the material behaviour being elasto-brittle-plastic.

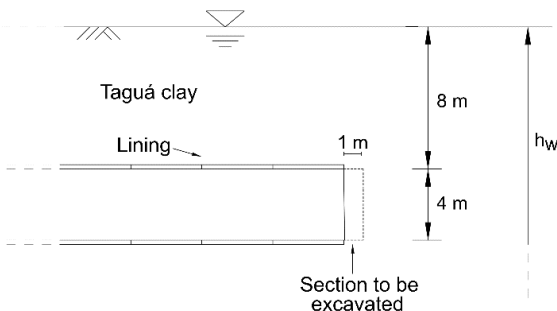


Figure 1 Cross section of the tunnel and excavation imposed

The soil mass was represented by a rectangular volume that was 36 m long (along the y axis), 32 m (x axis) wide, and 24 m high (z axis). These boundary dimensions were carefully chosen so as to not affect the results around the tunnel and to avoid any boundary effect. The tunnel was represented as a cylindrical volume that was 16 m long (parallel to x axis), 4 m in diameter, and at an 8 m depth from the surface. The unsupported excavation was represented as a third volume with the same diameter of the tunnel but with a 1 m length exactly in front of the tunnel face. Figure 2 presents the main dimensions of the model and the mesh created. The finite element mesh applied to the model was composed by four-noded tetrahedral elements (i.e. this element introduces nodes at the vertices of a tetrahedral shaped element) in a mesh of variable element size. The tetrahedral edges started with 0.3 m near the tunnel face and reached up to nearly 2.0 m at the boundaries of the model. The whole finite element mesh consisted of approximately 8,795 nodes and 49,157 elements.

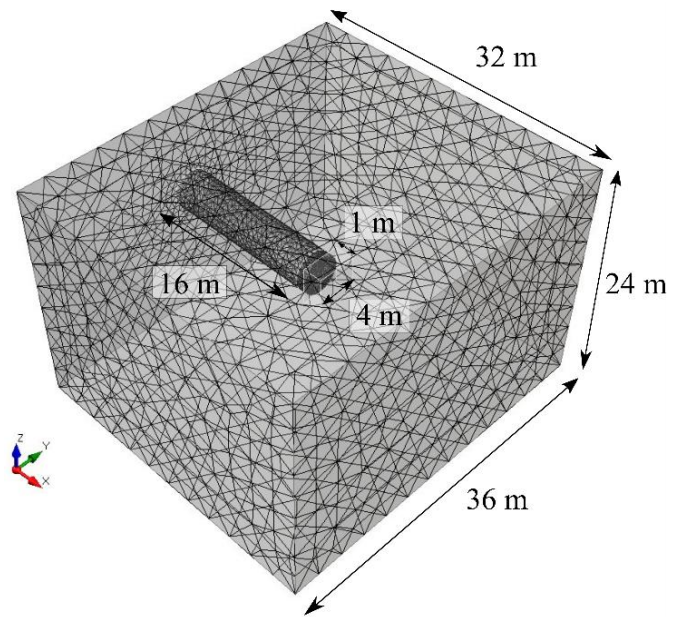


Figure 2 Three-dimensional element mesh and volume sizes of the model

The displacement boundary conditions adopted were as follows:

- The top of the external volume representing the soil mass was considered to be free to deform in all directions (x , y , and z), therefore, allowing for surface settlement.
- All the other boundaries of the external volume were fixed; all translation and rotations were restricted, and no deformation was allowed.
- The liner of the tunnel was simplified by imposing a boundary condition of no deformation in any direction (i.e. all nodal displacements at the tunnel wall are fixed). The introduction of a new variable in the model (i.e. the soil-liner interaction) was, therefore, avoided.
- The groundwater table was assumed to be well below the surface of the external volume, and it was assumed no variations during the excavation process (constant water table).
- The tunnel liner was considered waterproof; in other words, the water ingress into the tunnel was, therefore, not considered in the analysis.
- On the unsupported excavation volume, a free water boundary condition was applied. This allowed for an initially undrained condition (according to the soil permeability) and a drained condition afterwards.

To simulate the tunnel excavation sequence in the software, two phases were adopted:

- The first simulation phase involved determining the initial in-situ stress condition. The soils mass with a pre-existing full lined tunnel had its face sealed with a 0.3 m concrete wall with no mass (i.e. no unit weight value assigned) that was waterproof ($E = 300 \text{ GPa}$ and $\mu = 0.2$). During this phase, stress and hydrostatic equilibrium are statics, and there are no significant soil deformations toward the tunnel face (along x axis).
- The second phase involved removing the solid elements of the ground with the tunnel to simulate the tunnel excavation. Instantaneously, an excavation volume was added, which is a volume with no soil inside, and the wall that seals the tunnel face was removed. During this phase, there was stress relief associated with the excavation process, and tunnel face deformation was allowed along with water flux. The transition from the first phase to the second one was considered to have taken one second. The pore water pressure and soil displacement were inferred during specific times at predefined observation points. The pressure-displacement monitoring points were disposed in a set of five lines beginning from 10 cm of the excavation face of the tunnel and projecting itself toward the soil mass (Figure 3). Each line was 10 m long and contained 20 points disposed equally spaced along the x axis.

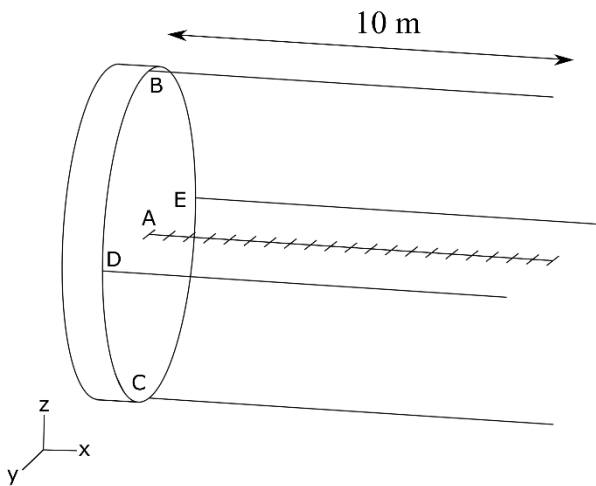


Figure 3 Layout and identification of the lines containing the observation points

4. THE PROPERTIES

The material properties used in the finite element simulation are of an overconsolidated stiff clay from São Paulo, southeastern Brazil, usually called Taguá. The Taguá clay is inserted in the context of the Resende Formation (Paleogene), which is about 80% in volume of the Sedimentary Basin of São Paulo, a rift basin housed in the Continental Rift of Southeastern Brazil (Riccomini, 2004). The sedimentary compounds of the Resende Formation are associated with alluvial fans that gradually change to river plains of braided rivers, with the Taguá clay corresponding mainly to distal deposits of the alluvial fans (Riccomini and Coimbra, 1992).

The mechanical properties of the Taguá clay have been studied in Brazil mainly for the construction of the underground railway system of the city of São Paulo. This system is in continuous improvement, which necessitates a better understanding of the behaviour of this material. Visually, Taguá clay is very similar to London clay as can be seen in Figure 4. Figure 4(a) shows an overview of a cut slope in Taguá clay where the cracks system created by shrinkage induce superficial failures. Figure 4(b) presents the fissured fabric of this clay, while Figure 4(c) shows another cut slope that depicts the

ongoing shrinkage process. Meanwhile, the association between the drying process and the original fractured structure can be seen in Figure 4(d).



Figure 4 Aspects of the Taguá clay from Resende Formation, Sedimentary Basin of São Paulo, São Paulo, Brazil

Taguá clay is a material with more than 70% of clay particles that are highly plastic, usually stiff, and with a greenish grey colour. Due to the evolution of the São Paulo sedimentary basin, marked by the erosion of some superficial layers, Taguá clay presents a $K_0 > 2$. (e.g. Ferreira et al., 1992; Massad, 2012). The soil water retention curves (SWRC) presented were obtained using undisturbed samples from a tunnel face of an ongoing excavation in Taguá clay in the city of São Paulo. The ϕ^b was estimated based on the model presented by Vilar (2006) and by using friction angle from literature. Details about the determination of the ϕ^b for the present case can be found in Vettorello (2019). Figure 5 presents results of tests performed with undisturbed specimens of Taguá clay and also data from London clay, for comparison. The SWRC was obtained by means of complementary methodologies that included a suction plate (until 30 kPa), pressure plate (40 to 500 kPa), and filter paper (> 500 kPa). A last point was inferred by allowing the specimen to air-dry and measuring the relative humidity of the air (suction = $-135055 \ln(\text{RH})$; Marinho, 1994).

In the finite element simulations, the soil was considered to behave as an elastic brittle plastic material (elasto-brittle-plastic) conforming to the Mohr-Coulomb failure criterion. The main parameters required in this constitutive model were as follows: cohesion (c'), friction angle (ϕ'), tensile strength (σ_t), residual friction angle (ϕ'_{res}), Poisson's ratio (μ), elastic modulus (E), and the dilation angle (ψ). The unit weight (γ), void ratio (e), and the coefficients of hydraulic conductivity (k) and lateral earth pressure (K_0) were also required as general parameters. As a parameter related with an unsaturated condition, the air-entry value ($u_a - u_w$)_b and the angle of soil shear strength change with suction (ϕ^b) were required. The parameters used for the analysis are given in Table 1. Aiming to evaluate the soil response with K_0 and k variation, more than one value was adopted for those parameters.

5. RESULTS AND DISCUSSIONS

Considering the undisturbed properties of the Taguá clay presented in Table 1 and the geometric characteristics of the model, a 1 m excavation advance from the tunnel was simulated. The excavation process caused changes in the stress state of the soil massif, and as a consequence, a negative variation of the pore water pressure within a certain volume of it was induced, particularly in the central portion of the face at the edge of the excavation (i.e. the *new* tunnel face).

The relationship between the pore water pressure developed due to stress relief of the excavation process and the distance from the

tunnel face for different times and for various hydraulic conductivity (k) along with the coefficient of earth pressure at rest (K_0) for the soil mass is illustrated in Figure 6. The observation points monitored are those disposed along the Line A of Figure 3 (centre of the tunnel face). In Figure 6(a) are presented the results for k of 10^{-6} m/s and K_0 of 2. In Figure 6(b), the results are for the same k value, but for a K_0 of 1. Complementary, these analyses were repeated, but for a lower value of k , and the results are presented in Figures 6(c) and 6(d), respectively.

It can be observed that the magnitude of the stress relief registered along Line A changes according to the K_0 value adopted. Comparing Figures 6(a) and 6(c), with 6(b) and 6(d), respectively, it is highlighted that when horizontal stresses are bigger than the vertical stress (i.e. $K_0 > 1$), the negative excess pore water pressure generated along the central portion of the tunnel face tends to be higher than when the massif stresses are isotropic (i.e. $K_0 = 1$). Negative excess pore water pressure ($-\Delta u_w$) was registered to extensions up to 10 m for all the analysed cases. However, suction ($-u_w$) was properly generated only along to smaller extensions, creating a *suction zone*. For the cases where $K_0 = 1$, no matter the k value, the *suction zone* occurred within the first meters from the tunnel face, which is about $\frac{1}{4}$ of the tunnel diameter. For the cases where $K_0 = 2$, the *suction zone* was of approximately 2 m, which is almost $\frac{1}{2}$ of the tunnel diameter.

The hydraulic conductivity in the analyses seems to act controlling the pore water dissipation rate; where the smaller is the value of k , the bigger is the time needed for a complete dissipation of the negative excess pore water pressure, and then, of the *suction zone*. As can be seen in Figures 6(c) and 6(d), the *suction zone* is maintained for more than 12 h, when $k = 10^{-8}$ m/s, although at this time the suction values registered are almost residual ($\approx 5\%$ or less of the maximum value). However, when $k = 10^{-6}$ m/s, the time needed for the same results to be reached is a few minutes or seconds (Figures 6(a) and 6(b), respectively).

The role of k in dissipating the negative excess pore water pressure is highlighted in Figure 7. Figure 7(a) illustrates the variation of the pore water pressure (Δu_w), right after the excavation (i.e. at 1 s) by the nearest observation point at the centre of the tunnel face (i.e.: 10 cm; Line A from Figure 3), according to different values of K_0 and k . For the same position, the resulting pore water pressure (u_w) is presented in Figure 7(b). The figures clearly show that the suction values registered right after the excavation tend to decrease with the increase of permeability. This behaviour suggests that medium to high permeability soils may not maintain the benefits in shear strength increase promoted by suction for long since the suction zone dissipates as quickly as the soil permeability increases. The tendency registered is similar for values of $K_0 = 1$ and 2.

The maximum suction value registered by the analyses was -168 kPa on the centre of the tunnel face (Figure 6(c)). This value is lower than the material air-entry value (approximately 1100 kPa), suggesting that at least for small diameters of excavation performed in the Taguá clay, the possibility of soil desaturation due to stress relief is not relevant. This is in agreement with the practice observed for tunnels excavated in Taguá clay. Usually, after the excavation processes, the tunnel face can be left open or just sealed with a layer of shotcrete for days, or even weeks. However, care must be taken for the development of cracks that may appear during this downtime. This aspect, however, was not considered in the present analysis.

As disused, the K_0 value has a great influence in the magnitude of the negative pore water pressure variation in the central area of the tunnel face. However, at the borders of the excavated face, the behaviour registered is different. Instead of a negative pore water pressure variation ($-\Delta u_w$), an almost instantaneous positive variation ($+\Delta u_w$) is detected resulting in an immediate soil yielding that increases with time towards the centre of the excavation. This phenomenon was monitored by the observation points disposed along the Lines B, C, D and E of Figure 3 (borders of the tunnel face) and can be viewed in Figure 8 for $K_0 = 1$ and $K_0 = 2$ after 1 s, 30 min, 1 h and 4 h of the excavation.

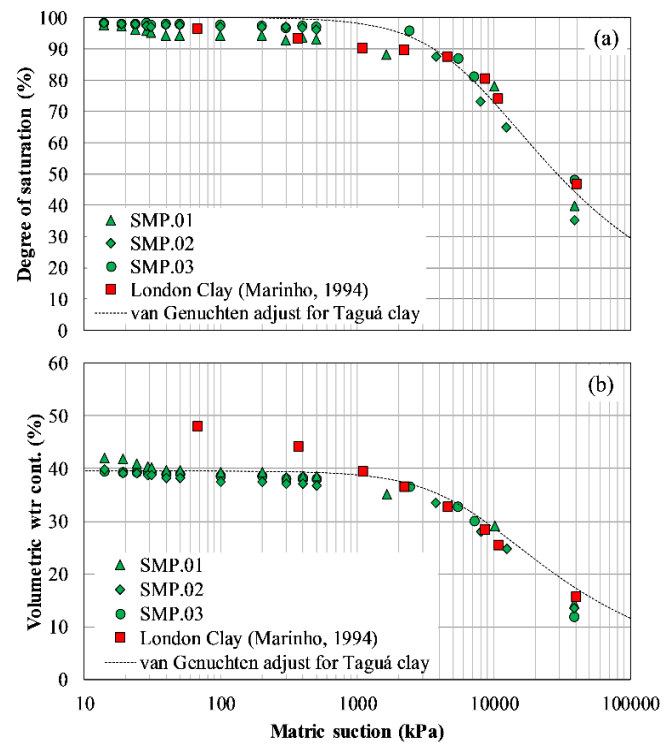


Figure 5 Soil water retention curve of the Taguá clay: (a) Matric suction versus degree of saturation, and (b) Matric suction versus volumetric water content

Table 1 Taguá clay parameters used in finite element analysis

Parameter	Value
γ (kN/m ³)	20.7
e	0.6
c' (kPa)	100
ϕ' (°)	21
σ_t (kPa)	0
ϕ'_{res} (°)	17
μ	0.2
E (Mpa)	200
ψ (°)	0
k (m/s)	$10^{-4}, 10^{-5}, 10^{-6}, 10^{-7},$ and 10^{-8}
K_0	1 and 2
$(u_a - u_w)_b$ (kPa)	1100
ϕ^b (°)	11.1

The mean stress (p') and pore water pressure (u_w) variation after the excavation process were also registered for the nearest observation point from the centre of the tunnel face (i.e.: 10 cm; Line A from Figure 3). Figure 9 presents the change in p' and u_w with time for $K_0 = 1$ and $K_0 = 2$ for two hydraulic conductivities. It can be observed that right after the excavation (i.e. 1 s), the pore water pressure registers an immediate drop of its values. However, the p' values, besides also registering a decrease tendency, do so at a slightly slower rate. This *delay* in p' values variation seems to be related to the process of negative excess pore water pressure dissipation and as expected, the smaller the soil permeability, the greater is the delay in the process of p' lowering.

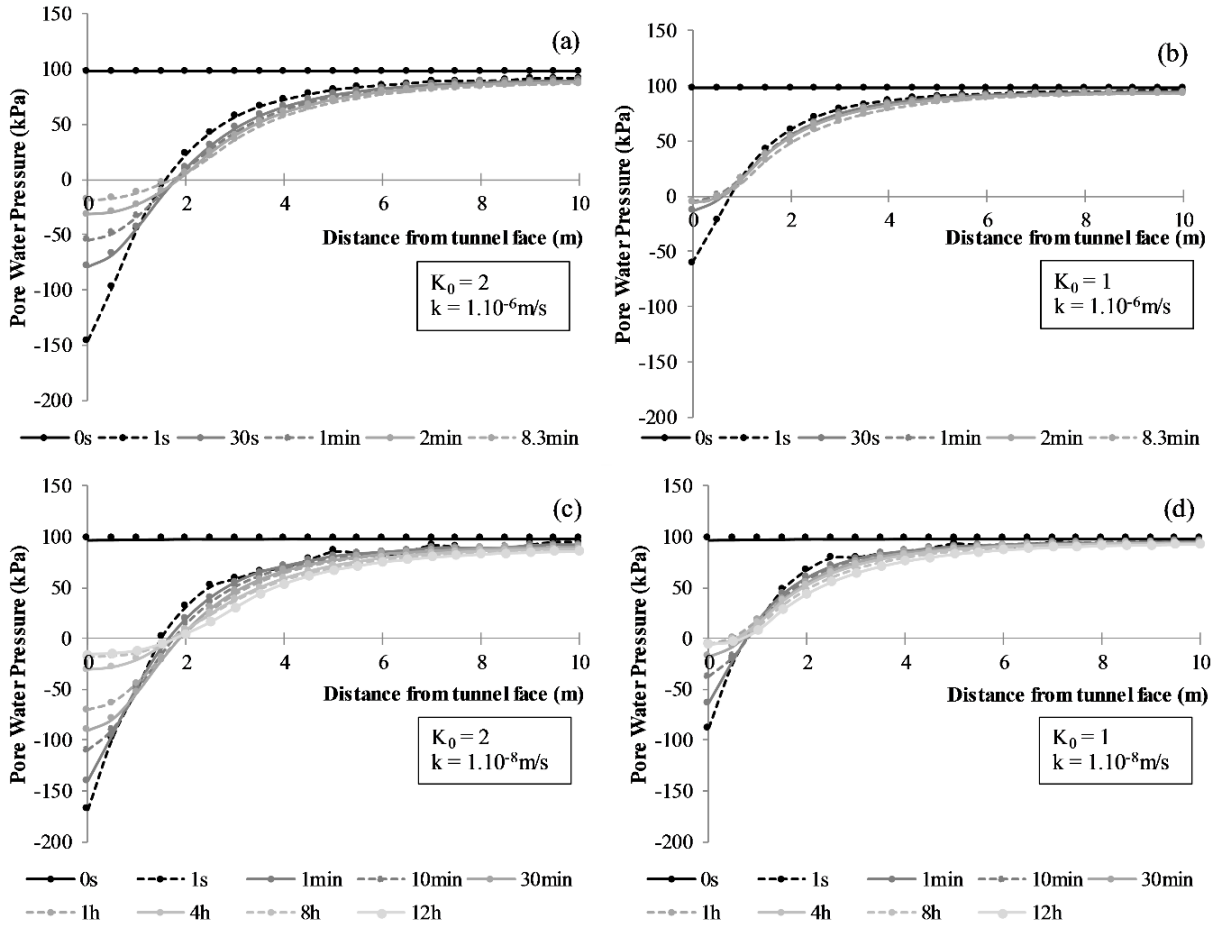


Figure 6 Pore water pressure developed due to stress relief, according to the distance from the tunnel face and for different times: (a) $k = 10^{-6}$ m/s and $K_0 = 2$, (b) $k = 10^{-6}$ m/s and $K_0 = 1$, (c) $k = 10^{-8}$ m/s and $K_0 = 2$, and (d) $k = 10^{-8}$ m/s and $K_0 = 1$

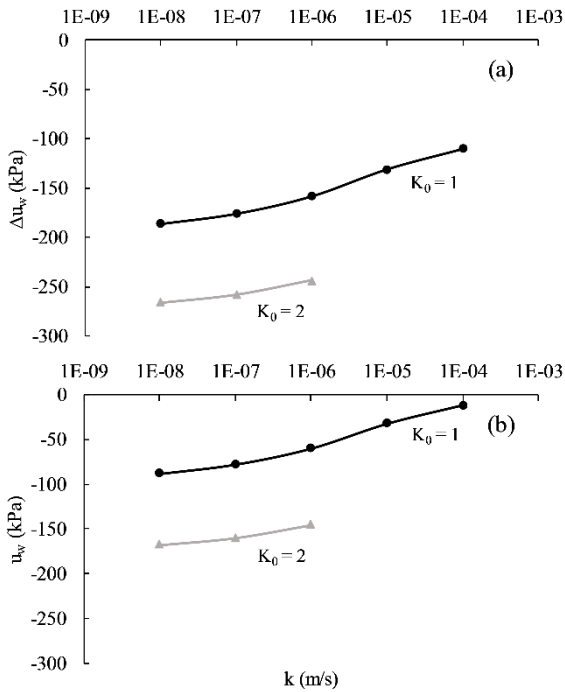


Figure 7 (a) Variation of the pore water pressure (Δu_w), and (b) Pore water pressure, registered at the centre of the tunnel face right after the excavation ($t = 1$ s), according to changes in the values of the coefficient of hydraulic conductivity (k) and K_0

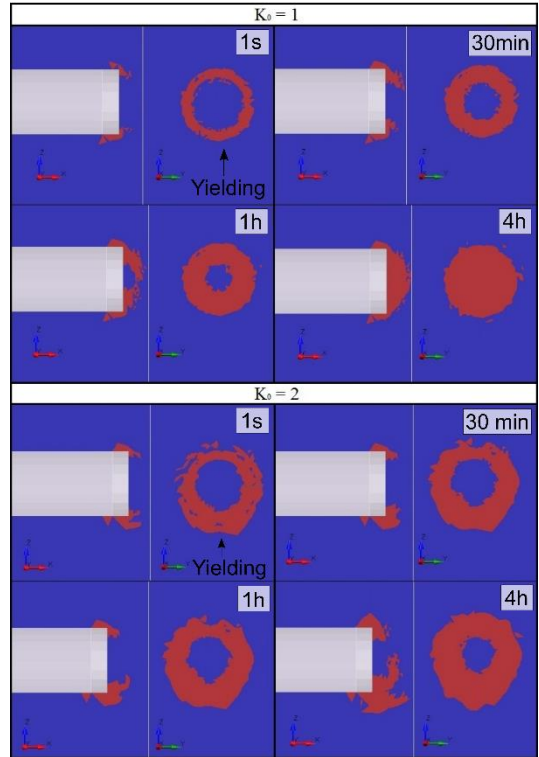


Figure 8 Soil yielding evolution after the excavation (planes xz and zy) for $K_0 = 1$ and 2

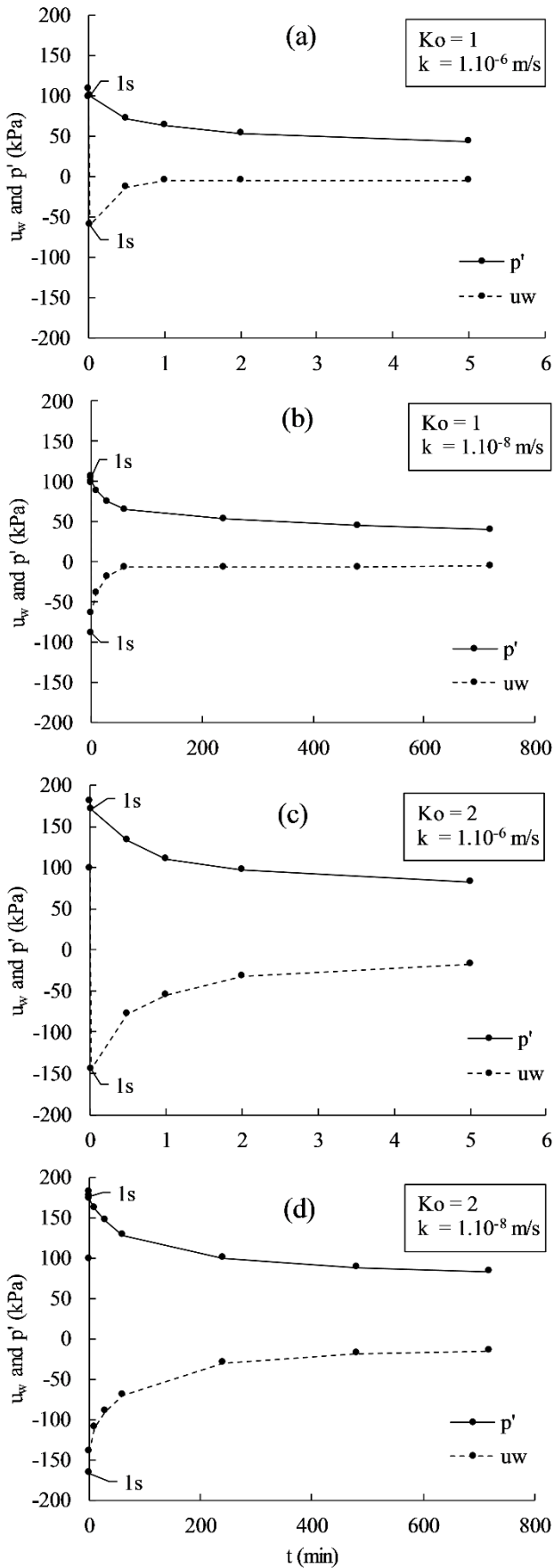


Figure 9 Pore water pressure (u_w) and mean effective stress (p') change with time at the nearest observation point from the centre of the tunnel face (i.e. 10 cm), where: (a) $K_0 = 1$ and $k = 1.10^{-6}$ m/s, (b) $K_0 = 1$ and $k = 1.10^{-8}$ m/s, (c) $K_0 = 2$ and $k = 1.10^{-6}$ m/s, and (d) $K_0 = 2$ and $k = 1.10^{-8}$ m/s

Figure 10 illustrates the time needed for specific displacements to occur in the tunnel (along the x axis) for different values of hydraulic conductivity. For $K_0 = 2$, the displacement along the x axis (normal to tunnel face) tends to occur slightly faster than in case where $K_0 = 1$ for bigger displacement values. For a displacement of 10 mm, the time is shorter when $K_0 = 2$ than when $K_0 = 1$ and decreases from 42 to 38 hours, respectively. This gap, however, tends to decrease for small displacement values, such as for a 4 mm displacement where for both values of K_0 , the time needed for the deformation to occur is about four hours.

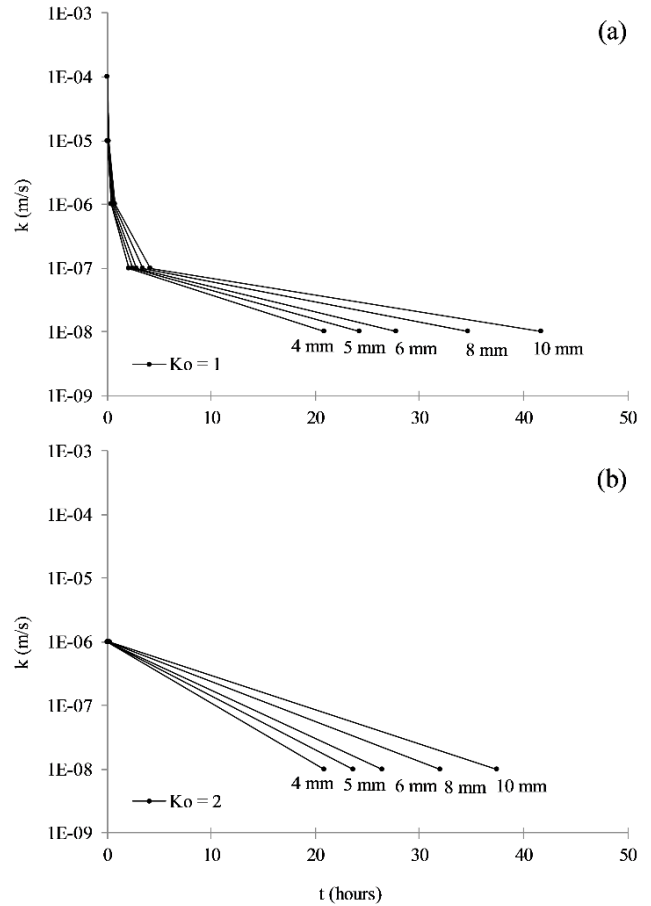


Figure 10 Effect of k on the time needed for a specific displacement to occur into the excavation along the x axis (normal to the tunnel face), considering the closest observation point at the centre of the tunnel face (i.e. 10 cm), where: (a) $K_0 = 1$ and (b) $K_0 = 2$

The stress paths of the analyses for the nearest observation point from the centre of the tunnel face have been reconstituted for the time immediately after excavation (i.e. 1 s) from 10 s to 12 h according to the material permeability. The results are shown in Figures 11(a) and 11(b), for $K_0 = 1$ and $K_0 = 2$, respectively.

For the case where $K_0 = 1$ (Figure 11(a)), there is a strong increase in the value of the deviatoric stress (q), and a reduction in the effective mean stress (p'). It should be noted that the negative pore pressures generated do not desaturate the material and so the principle of effective stresses is valid. In the same figure, it is observed that the greater the hydraulic conductivity, the greater the value of q , and the lower the value of p' , right after the excavation. This means that with the permeability increase, the resulting stress state tends to be closer to the yielding condition. Immediately after the excavation and for $k = 10^{-8}$ m/s, the mean effective stress (p') reduced to about 3% (108 to 103 kPa) while it is approximately 37% (108 to 68 kPa) when $k = 10^{-4}$ m/s, highlighting the influence of the hydraulic conductivity as a conditioning factor in soil deformation rate. In terms of displacements, for $K_0 = 1$, it is observed that immediately after the excavation (i.e. 1 s), the displacements vary from 2.8 mm, when

$k = 10^{-4}$ m/s, to 1.9 mm, when 10^{-8} m/s, which indicates that the hydraulic conductivity has some influence on the value of the displacement at the first moment. Moreover, when $k = 10^{-4}$ m/s, the instantaneous displacement promoted is almost plastic (i.e. very close to the yielding point) which may bring the soil to a state closer to failure.

For the case of $K_0 = 2$ (Figure 11(b)), only two values of hydraulic conductivity were analyzed since it is unlikely that a soil over consolidated would have high values of hydraulic conductivity. In this case, a small reduction in q is observed along with a decrease in p' . The levels of displacements obtained for $K_0 = 2$ indicate that even if the over consolidated soil reaches the same displacement values, the material (at the analysed point) would not reach the yielding point.

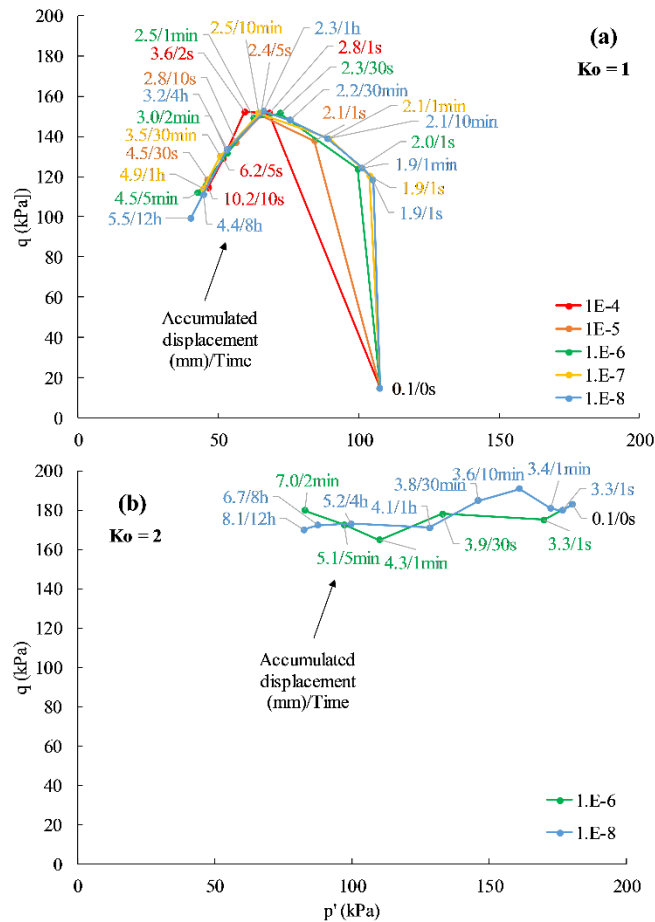


Figure 11 Failure envelop considering data registered by the nearest observation point from the centre of the tunnel face (i.e. 10 cm) over time for different values of k and K_0 : (a) $K_0 = 1$ and (b) $K_0 = 2$

Based on the time needed for the soil to reach the yielding point for some values of hydraulic conductivity, it was possible to develop the graph presented in Figure 12. This graph, however, considers only the evolution of the nearest observation point at the centre of the tunnel face (i.e.: 10 cm; Line A from Figure 3), when $K_0 = 1$. The data for $K_0 = 2$ were not plotted since the yield point was not reached for the analysis time. Besides being a very specific case, Figure 12 may illustrate the influence of the pore water pressure dissipation rate on soil yielding. The results highlight that the lower the hydraulic conductivity, the longer the yielding time. As can be noted, a yielding time of 60 min is observed for a hydraulic conductivity of 10^{-8} m/s; on the other hand, for values less than 10^{-7} m/s, the time taken is less than 10 min.

6. CONCLUSIONS

The change in pore water pressure due to an excavation of an unsupported segment of soil within a shallow and low diameter tunnel

was studied by means of a coupled and transient numerical analysis by using a 3D mesh. The study aimed to simulate the behaviour of stiff soil from the city of São Paulo (southeastern Brazil) and also perform a parametric analysis varying the massif stress state (k_0) and hydraulic permeability (k).

The main conclusions of the study can be summarized as follows:

- The excavation process does not always induce a general stress relief. However, there is a clear tendency to reduce the pore water pressure in the centre of the tunnel face. The higher the value of K_0 , the higher is the reduction in pore water pressure, which, in some cases, generates suction (negative pore water pressure).
- This behaviour was not confirmed when the borders of the tunnel face were considered. However, the tendency of the pore water pressure lowering right after the excavation is preceded by an immediate pore water pressure increase resulting in soil yielding.
- The decrease of the pore water pressure due to excavation may promote the development of a suction zone in front of the tunnel face. The extent of this region right after the excavation as its dissipation rate through time depend on the magnitude of the stress relief, which is highly influenced by the K_0 value and the water permeability, respectively.
- Inside the suction zone, the soil shear strength is increased and, as a consequence, the soil yielding is delayed.
- Considering the tunnel geometry and depth, the excavation did not generate soil desaturation, since the suction generated did not exceed the soil air-entry value. Soil desaturation may lead to a change in the interpretation of the effective stresses and deformation rate of the soil highlighting that there is valuable information the water retention curve may bring to this sort of analysis.

The results presented highlight the potential application of suction as a parameter in the stability analysis of horizontal excavations. However, overconsolidated materials with low hydraulic conductivity, such as the Taguá clay, are the ones that may reap better benefits from suction increase in terms of soil shear strength. The incorporation of this factor during stability analysis may help developing more realistic numerical models and, as a consequence, allow for a better determination of time and for the excavation span to remain unsupported.

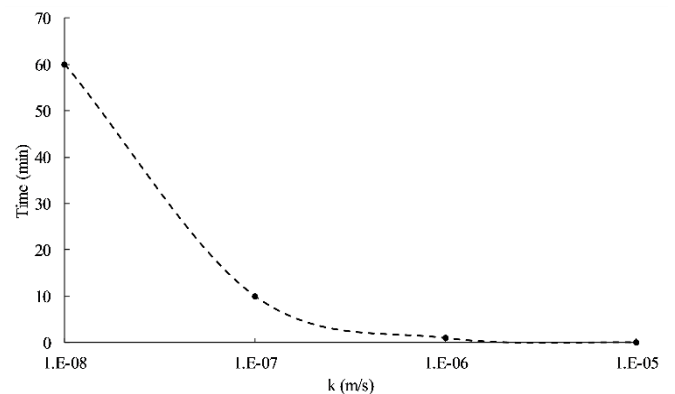


Figure 12 Time needed for Taguá clay to yield after excavation at the nearest observation point from the centre of the tunnel face (i.e. 10 cm) according to the hydraulic conductivity when $K_0 = 1$

7. ACKNOWLEDGEMENTS

The authors would like to thank the Coordenação de Aperfeiçoamento de Pessoal de Nível Superior - Brasil (CAPES – Coordination for the Improvement of Higher Education Personnel | Finance Code 001), which partly financed this study and the Instituto

de Pesquisas Tecnológicas do Estado de São Paulo (IPT-SP – Institute for Technological Research of São Paulo), in cooperation with its foundation (FIPT-SP), for their financial and institutional support through the Novos Talentos program.

8. LIST OF NOTATIONS

c'	effective cohesion
e	void ratio
E	Young's modulus
h_w	pressure head
k	coefficient of hydraulic conductivity
K_0	coefficient of earth pressure at rest
p'	mean effective stress
q	deviatoric stress
RH	relative humidity
u_w	porewater pressure
Δu_w	excess pore water pressure
$(u_a - u_w)_b$	air-entry value
ϕ'	angle of internal friction
ϕ^b	angle of soil shear strength change with suction
ϕ_{res}	residual angle of internal friction
γ	natural specific weight of the soil
μ	Poisson's ratio
σ_t	tensile strength
ψ	dilatancy angle

9. REFERENCES

- Biot, M. (1941) "General Theory of Three-Dimensional Consolidation. Journal of Applied Physics", 12(2), pp155–164.
- Davis, E., Gunn, M., Mair, R., and Seneviratne, H. (1980) "The stability of shallow tunnels and underground openings in cohesive material", *Géotechnique*, 30(4), pp397–416.
- Ferreira, A., Alonso, U., and Luz, P. (1992) "Solos da Cidade de São Paulo", São Paulo: Associação Brasileira de Mecânica dos Solos (ABMF) and Associação Brasileira de Empresas de Engenharia (ABEF) (in Portuguese).
- Höfle, R., Fillibeck, J., and Vogt, N. (2008) "Time dependent deformations during tunnelling and stability of tunnel faces in fine-grained soils under groundwater", *Acta Geotechnica*, 3(4), pp309–316.
- Holt, D., and Griffiths, D. (1992) "Transient analysis of excavations in soil", *Computers and Geotechnics*, 13(3), pp159–174.
- Kovacevic, N., Hight, D., and Potts, D. (2007) "Predicting the stand-up time of temporary London Clay slopes at Terminal 5, Heathrow Airport", *Géotechnique*, 57(1), pp63–74.
- Marinho, F. (1994) "Shrinkage Behaviour of Some Plastic Soils", Ph.D. thesis, University of London.
- Marinho, F., Standing, J., and Kuwagima, R. (2003) "Soil suction development under isotropic loading and unloading in a compacted residual soil", *Soils and Rocks*, 26(2), pp115–128 (in Portuguese).
- Massad, F. (2012) "Resistência ao cisalhamento e deformabilidade dos solos sedimentares de São Paulo", In: *Seminário Twin Cities: Solos das regiões metropolitanas de São Paulo e Curitiba*. São Paulo: Associação Brasileira de Mecânica dos Solos e Engenharia Geotécnica (ABMS), pp107–133 (in Portuguese).
- Ng, C., and Lee, G. (2002) "A three-dimensional parametric study of the use of soil nails for stabilising tunnel faces", *Computers and Geotechnics*, 29(8), pp673–697.
- Potts, D., Kovacevic, N., and Vaughan, P. (1997) "Delayed collapse of cut slopes in stiff clay", *Géotechnique*, 47(5), pp953–982.
- Riccomini, C., and Coimbra, A. (1992) "Geologia da Bacia Sedimentar", In: *Solos da Cidade de São Paulo*. São Paulo: Associação Brasileira de Mecânica dos Solos (ABMF) and Associação Brasileira de Empresas de Engenharia (ABEF), pp37–94 (in Portuguese).
- Riccomini, C., Sant'Anna, L., and Ferrari, A. (2004) "Evolução geológica do Rift Continental do Sudeste do Brasil", In: V. Mantesso-Neto, A. Bartorelli, C. Carbeiro and B. Neves, ed., *Geologia do Continente Sul-Americano: Evolução da obra de Fernando Flávio Marques de Almeida*, 1st ed. São Paulo: Beca, pp385–405 (in Portuguese).
- Rocscience (2019) "RS3 - Version 3.005", Toronto, Ontario, Canada: Rocscience INC.
- Schuerch, R., and Anagnostou, G. (2013) "Analysis of stand-up time of the tunnel face", In: *Proceedings of the 39th World Tunnel Congress*. Geneva, Switzerland, pp709–714.
- Simonsen, T., and Sorensen, K. (2017) "Field measurements of pore-water pressure changes in a stiff fissured very high plasticity Paleogene clay during excavation and pile driving", In: *Proceedings of the 19th International Conference of Soil Mechanics and Geotechnical Engineering*. Seoul, South Korea, pp2865–2868.
- Terzaghi, K. (1923) "Die berechnung der durchlassigkeitsziffer des tones aus dem verlauf der hydrodynamischen spannungerscheinungen", *Mathematisch-naturwissenschaftliche, Klasse. Akademie der Wissenschaften*, Vienna, pp125–138 (in German).
- Terzaghi, K. (1950) "Geological aspects of soft-ground tunneling", In: P. Trask, ed., *Applied sedimentation*, 1st ed. New York: Wiley, pp193–209.
- Vanapalli, S., Fredlund, D., Pufahl, D., and Clifton, A. (1996) "Model for the prediction of shear strength with respect to soil suction", *Canadian Geotechnical Journal*, 33(3), pp379–392.
- Vaughan, P., and Walbancke, H. (1973) "Pore pressure changes and the delayed failure of cutting slopes in overconsolidated clay", *Géotechnique*, 23(4), pp531–539.
- Vettorello, D. (2019) "Avaliação Dos Efeitos Do Alívio De Tensões No Desenvolvimento De Poropressões De Água Em Obras Subterrâneas Em Solos", M.A. Dissertation, Universidade de São Paulo (in Portuguese).
- Vilar, O. (2006) "A simplified procedure to estimate the shear strength envelope of unsaturated soils", *Canadian Geotechnical Journal*, 43(10), pp1088–1095.
- Wan, M., and Standing, J. (2014) "Field measurement by fully grouted vibrating wire piezometers", *Proceedings of the Institution of Civil Engineers - Geotechnical Engineering*, 167(6), pp547–564.